Predicted electrical properties of modulation-doped ZnO-based transparent conducting oxides

D. J. Cohen and S. A. Barnett[a)]
Department of Materials Science and Engineering, Northwestern University, Evanston, Illinois 60208

(Received 15 March 2005; accepted 21 July 2005; published online 8 September 2005)

A one-dimensional Poisson/Schrödinger program has been used to predict the effect of layer thicknesses, donor concentration, and band-gap offset on the electrical properties of transparent conducting modulation-doped ZnO/ZnMgO multilayer structures. Mobilities as high as 145 $cm^2/V\,s$ were predicted for a structure with an average carrier density of 3.8×10^{18} cm^{-3} and a resistivity of 1×10^{-2} Ω cm; for a comparable resistivity in monolithic ZnO, the mobility would be lower ~30 $cm^2/V\,s$ and the carrier density would be higher, leading to higher optical absorption. However, it was found that the maximum sheet electron density that could be transferred from the doped to the undoped layers was $\sim10^{13}$ cm^{-2}, limiting the lowest calculated resistivity to $\sim1.5\times10^{-3}$ Ω cm. The optimal thicknesses to simultaneously achieve high mobility and low resistivity were 2–5 nm for both the pure ZnO and ZnMgO:Al layers. For ZnO thicknesses above this range the resistivity steadily increased, and below 2 nm the mobility decreased. For ZnMgO:Al thicknesses increased above this range, the mobility rapidly decreased, whereas decreasing below 2 nm increased the resistivity. The effect of the pure ZnMgO set-back layer thickness on mobility is discussed and a spacer layer of ~1.5 nm is proposed for ZnO/ZnMgO multilayers. The effect of ZnO layer thickness on possible intersubband scattering is also discussed. © *2005 American Institute of Physics*. [DOI: 10.1063/1.2035898]

I. INTRODUCTION

Transparent conductive oxides (TCOs) are utilized as electrodes in technologically important applications such as flat panel displays[1] and solar cells.[2] The development of larger screen sizes, higher-efficiency photovoltaic cells, and transparent electronics[3–5] creates a need for TCO materials with improved properties, particularly lower resistivity and higher transparency. Recent attempts to decrease the resistivity $\rho=(ne\mu)^{-1}$ have typically focused on increasing the mobility μ rather than the carrier concentration n (e is the electron charge). This is because increasing n above a certain level leads to diminishing returns: decreased mobility due to ionized impurity scattering[6] and decreased transparency due to free-carrier absorption.[7] The mobility $\mu=e\tau/m^*$ can be increased by increasing the relaxation time τ or by decreasing the effective mass m^*. Recently, TCO materials with lower effective masses and improved crystal quality, in order to increase τ, have been developed.[8–10] There is also an interest in achieving high-mobility layers for transparent field-effect transistors.[11]

One proposed method for increasing τ in TCOs is by using modulation-doped multilayer films.[12,13] In this method, donor atoms are placed in wider band-gap layers and the resulting conduction-band electrons transfer across the heterojunction interfaces to undoped, smaller band-gap layers. Since the electrons are confined in the undoped layers, there is minimal scattering by ionized impurities. While modulation doping has been successfully used to increase mobilities in many semiconductor systems including GaAs/AlGaAs,[14,15] GaN/AlGaN,[16] and Si/SiGe,[17] it has not been demonstrated in TCOs. The parameters defining modulation-doped multilayer structures, including layer thicknesses, compositions, and doping levels, must be chosen such that complete charge transfer from the doped to the undoped layers is achieved at high electron densities typical of TCO films. There is a need for a simulation tool that will provide information on the structural dimensions that can best achieve effective electron transfer and high mobility. Calculations were recently reported predicting enhanced electronic properties of modulation-doped oxides.[18] However, these calculations assumed generalized oxide properties, did not vary all of the key multilayer parameters, and did not consider the requirements for multilayer growth, e.g., lattice match between layers.

In this paper, one-dimensional Poisson/Schrödinger simulations have been carried out for a proposed TCO modulation-doped system: ZnO/ZnMgO. The advantages of this system include reasonable lattice match (good quality ZnMgO epitaxial growth has already been demonstrated)[19] and many of the parameters needed for the calculation, e.g., band gaps and effective masses,[19] have been measured. Thus, fairly realistic results can be expected from the calculation. The effect of layer thicknesses, donor concentration, and band-gap offset on the simulated electrical properties are presented.

II. SIMULATION PROCEDURE

The simulation program, developed by Snider,[20] uses the method of finite differences to self-consistently solve the one-dimensional Poisson and Schrödinger equations.[21] The number of mesh points used for each simulation was 500,

[a)]Electronic mail: s-barnett@northwestern.edu

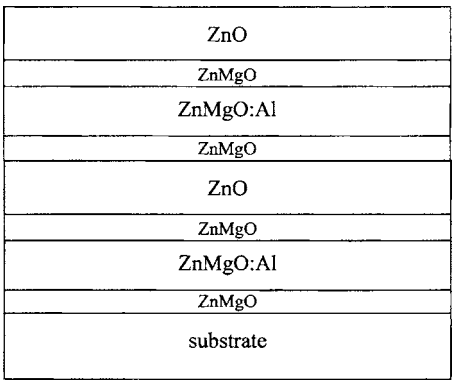

FIG. 1. Schematic diagram showing two periods of the simulated modulation-doped multilayer structure.

which corresponds to a mesh spacing between 0.27 and 0.071 nm. The boundary conditions used in the simulations were to set the slope of the bands equal to zero at the substrate and the surface. The output of the program includes the conduction and valence bands, electron distribution, and the wave functions for confined states.

Figure 1 shows a schematic diagram of the simulated multilayer structure. The ZnMgO, which has a larger band-gap than ZnO,[22] is donor-doped with aluminum to provide excess electrons.[19,23] The aluminum was assumed to be fully ionized. Undoped ZnMgO spacer layers separate undoped ZnO layers and the ZnMgO:Al layers. The values of the variables used in the calculations are given in Table I. The band gap, effective mass, and mobility values for the ZnMgO layers are based on experimental results for 20 at. % Mg films.[19] The heterojunction between ZnO and ZnMgO is assumed to have type-I alignment with the difference in the band-gap evenly divided between the conduction-band offset and the valence-band offset.[24] X-ray photoelectron spectroscopy (Omicron ESCA Probe) was performed on ZnO/ZnMgO samples grown in our laboratory by dc-reactive magnetron sputtering to estimate the conduction-band offset at the heterointerface.[25] While there was a relatively large uncertainty in the measured position of the valence-band edge, the results were consistent with equal valence- and conduction-band offsets, as used in the simulations.

Overall mobility values (for conduction parallel to the layers) were calculated by averaging the mobilities expected for each layer weighted by the predicted electron distributions. Table I shows the individual layer carrier concentration and the mobility values used in the calculations. A mobility of 200 $cm^2/V\,s$, the value for pure bulk single-crystal ZnO,[26] was assumed for electrons in the pure ZnO layers. The thickness of the undoped ZnMgO layer was set at 1.5 nm; as discussed in Sec. IV, this thickness was chosen in order that ZnO mobilities would not be reduced by remote ionized impurity scattering. The mobility for ZnMgO, 5 $cm^2/V\,s$, was a previously measured experimental value.[19,27] The carrier concentration in the undoped ZnO and ZnMgO layers was set at 1×10^{15} cm^{-3}. The static dielectric constant for all layers was set to 8.5.[28] The temperature was set to 300 K for all of the simulations. All mobility, carrier density, and resistivity values quoted below are averages over the entire multilayer structure.

TABLE I. Summary of material properties used in the simulations unless otherwise indicated.

Material	Band gap (eV)	Conduction-band offset (eV)	Effective mass ($/m_o$)	Mobility ($cm^2/V\,s$)
ZnO	3.3	0	0.38[a]	200
ZnMgO	3.8	0.25	1.5	5
ZnMgO:(Al)	3.8	0.25	1.5	5

[a]Reference 37.

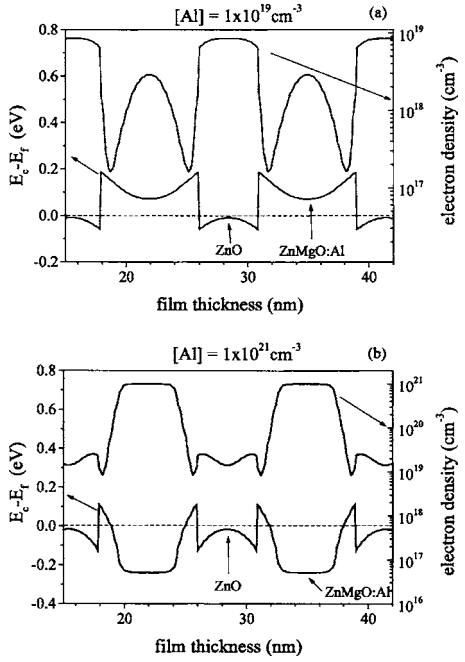

FIG. 2. Calculated electron densities and conduction band positions for ZnMgO:Al doping densities of 1×10^{19} (a) and 1×10^{21} cm^{-3} (b). The layer thickness values used are ZnMgO:Al=5 nm, ZnMgO=1.5 nm, and ZnO =5 nm. The dashed line represents the position of the Fermi level.

III. RESULTS

Figure 2 shows the carrier concentration profiles and conduction-band diagrams for typical structures: ZnMgO:Al thickness of 5 nm with $[Al]=1\times10^{19}$ cm^{-3} (a) and $[Al]=1\times10^{21}$ cm^{-3} (b), ZnO thickness of 5 nm, and ZnMgO thickness of 1.5 nm. For $[Al]=1\times10^{19}$ cm^{-3}, the conduction band shows the band bending typical of modulation doping, with energy minima at the edges of the pure ZnO layer. For $[Al]=1\times10^{21}$ cm^{-3}, local minima are still present, but they are actually at a higher energy than in the ZnMgO:Al layer. This results from the space-charge density from the transfer of a large electron density from the ZnMgO:Al layers into the ZnO. The electron distributions within the layers are quite different for the two doping levels. For $[Al]=1\times10^{19}$ cm^{-3}, the electrons transfer into the ZnO layers up to a level of $\sim8\times10^{18}$ cm^{-3}, and the carrier concentration in the ZnMgO:Al layers falls to $\sim2\times10^{18}$ cm^{-3}. That is, $\sim$88% of the electrons from the ZnMgO:Al layer are transferred to the ZnO and ZnMgO layers. Rather than forming a two-dimensional electron gas at the interfaces, there is a

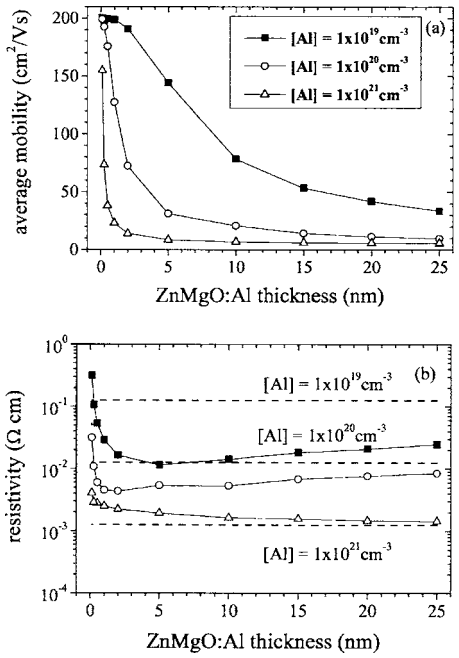

FIG. 3. The effect of doped layer thickness and donor concentration on the average multilayer mobility (a) and resistivity (b). The ZnO thickness is 5 nm and the ZnMgO thickness is 1.5 nm. The dashed lines in (b) represent the resistivities expected for the ZnMgO:Al layers at each donor concentration.

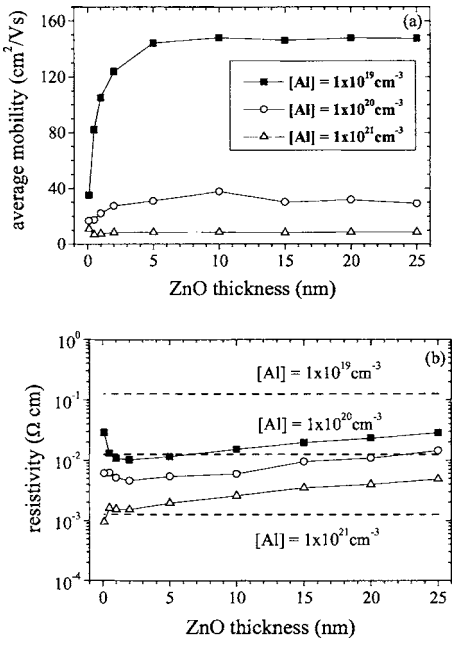

FIG. 4. The effect of ZnO layer thickness and donor concentration on the average multilayer mobility (a) and resistivity (b). The ZnMgO:Al thickness is 5 nm and the ZnMgO thickness is 1.5 nm. The dashed lines in (b) represent the resistivities expected for the ZnMgO:Al layers at each donor concentration.

fairly uniform electron density throughout the ZnO layer. This results because the ZnO layer is relatively thin and electron sheet densities are relatively high. As the doping density is increased, larger electron densities [note that the ZnO electron density is much higher in Fig. 2(b) than Fig. 2(a)] result in space charge that raises energy levels, thereby limiting further electron transfer. For example, in the [Al] $=1\times10^{21}$ cm^{-3} case only $\sim$8% of the electrons are transferred from the ZnMgO:Al. This shows an important trend: a limited number of electrons can be transferred between layers because of the space charge that builds up between transferred electrons and their ionized donors.

Figure 3 shows the effect of the ZnMgO:Al layer thickness and donor concentration on the average mobility [Fig. 3(a)] and the resistivity [Fig. 3(b)]. For all of the simulation results in Fig. 3, the ZnO thickness was 5 nm and the ZnMgO thickness was 1.5 nm. In Fig. 3(a) for a ZnMgO:Al layer thickness of 5 nm (the value used in Fig. 2), the mobility decreases from $\sim$150 cm^2/V s for an Al doping level of 10^{19} cm^{-3} to $\sim$10 cm^2/V s for an Al doping level of 10^{21} cm^{-3}. The higher mobility at the lower Al content reflects the efficient electron transfer to the high-mobility ZnO layer, whereas the higher electron density is mostly retained in the low- mobility ZnMgO:Al layer (Fig. 2). In general, as the ZnMgO:Al layer thickness decreased, the average multilayer mobility increased, as it was possible to transfer a greater fraction of the electrons. Based on Fig. 3(a) there is a critical electron sheet density for efficient electron transfer. Typically, an average multilayer mobility of $\geqslant$150 cm^2/V s was achieved for electron transfer of $\geqslant$88%, which occurred for electron sheet densities $\leqslant10^{13}$ cm^{-2}.

Figure 3(b) shows that the overall multilayer resistivity decreases as the donor concentration increases. The dashed lines in Fig. 3(b) indicate the resistivity that would be expected for monolithic ZnMgO:Al layers for each donor concentration. For the lower Al doping levels, modulation doping substantially decreases the resistivity, primarily because of the high mobility achieved. The resistivity decreases as the doped layer thickness decreases, reaching a minimum at $\sim$5 nm for an Al doping level of 10^{19} cm^{-3}, due to the increase in mobility shown in Fig. 3(a). Further decreases in doped layer thickness result in an increase in resistivity, despite increasing mobility, due to the decreasing fraction of the structure that is doped. For the highest Al doping concentration, the mobility increases only for very small doped layer thicknesses, and no resistivity decrease was observed.

The effect of ZnO layer thickness on the average mobility is shown in Fig. 4(a) and on multilayer resistivity in Fig. 4(b). The ZnMgO:Al thickness is 5 nm and the ZnMgO thickness is 1.5 nm. High mobilities were achieved for lower Al concentrations, with the low mobilities at higher Al concentrations again due to ineffective electron transfer as in Fig. 3(a). There was little effect of ZnO thickness above 5 nm on the mobility, but below 5 nm the mobility decreased. This was explained by a rapid decrease in the number of confined electron states with decreasing ZnO thickness, which limited the density of electrons that could be transferred to the ZnO, thereby limiting the mobility. For example, the wave-function calculations showed no confined states for ZnO thickness $<1-2$ nm for ZnMgO:Al doping densities of $10^{19}-10^{20}$ cm^{-3}. The multilayer resistivity [Fig. 4(b)] decreases as the ZnO thickness decreases down to $\sim$2 nm due to the decreasing fraction of undoped material (higher average doping density). The resistivity increase for thickness decreased below 2 nm is explained by the mobility

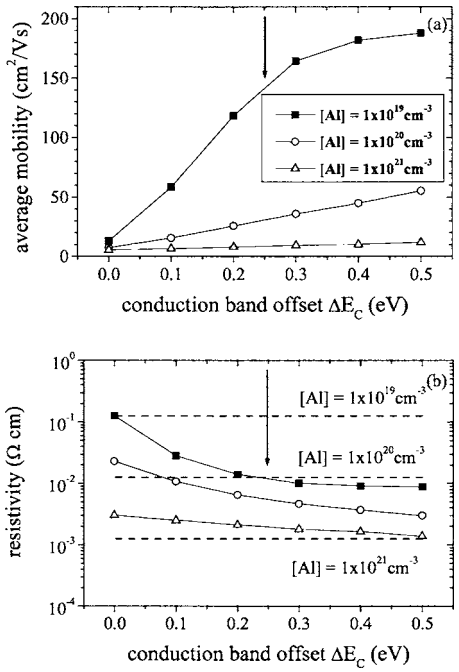

FIG. 5. The effect of conduction-band offset ΔE_C and donor concentration on the average mobility (a) and resistivity (b). The ZnO thickness is 5 nm, the ZnMgO:Al thickness is 5 nm, and the ZnMgO thickness is 1.5 nm. The dashed lines in (b) represent the resistivities expected for the ZnMgO:Al layers at each donor concentration. The arrows indicate the offset value used in other calculations in this paper.

decrease shown in Fig. 4(a). The dashed lines in Fig. 4(b) represent the resistivity of the ZnMgO:Al layers for each donor concentration. The multilayers with lower donor concentrations show a greater improvement in resistivity when compared to the resistivity of the ZnMgO:Al layer by itself [dashed lines in Fig. 4(b)].

The lowest resistivity value obtained in these simulations was 1.21×10^{-3} Ω cm for a multilayer with 1-nm-thick ZnO and ZnMgO:Al layers and an Al concentration of 10^{21} cm^{-3}. In this case, however, the mobility was only $\sim$20 cm^2/V s. Further improvements with decreased layer thicknesses were not possible owing to the low average mobility of the multilayer when the ZnO thicknesses were small.

In the above calculations, the conduction-band offset ΔE_C was taken to be $\Delta E_G/2$, or 0.25 eV assuming $Zn_{0.8}Mg_{0.2}O$. However, the actual offset may be different based on a different alloy composition or if the offset is actually a different fraction of the band gap. Thus, we have explored the effect of ΔE_C on the average mobility [Fig. 5(a)] and the resistivity [Fig. 5(b)]. As shown in Fig. 5, the mobility increases and resistivity decreases as ΔE_C increases. The influence of ΔE_C on the average mobility is more pronounced at lower donor concentrations, indicating a greater efficiency in the transfer of electrons from the ZnMgO:Al layers to the ZnO layers. Above $\sim$0.3 eV the average mobility for the [Al]$=1\times10^{19}$ cm^{-3} series tends to level out as the mobility value approaches the ZnO value of 200 cm^2/V s, indicating 100% electron transfer. As a result, further increases in ΔE_C will not significantly improve the electron concentration in the ZnO layers. The changes in resistivity with ΔE_C along with the resistivity values of the ZnMgO:Al layers by themselves (dashed lines) are shown in Fig. 5(b). Once again, the improvement in the resistivity as a result of the multilayer structure is most pronounced at lower donor concentrations.

IV. DISCUSSION

The simulations in this work provide insight into the possibility of using ZnO/ZnMgO modulation-doped TCOs. In order to compete with existing TCOs for applications such a flat panel displays and solar cells, it is necessary to achieve a low resistivity. Based on Figs. 3(b) and 4(b) the lowest resistivity can be achieved when the ZnMgO:Al and ZnO layers are less than 5 nm. In our simulations we found that the multilayer structures had lower resistivities than their constituent monolithic layers [dashed horizontal lines in Figs. 3(b) and 4(b)] at low donor concentrations. For a donor concentration of 1×10^{21} cm^{-3} the resistivity approaches the monolithic limit when the ZnO thickness is 2 nm [Fig. 4(b)]. This result is in agreement with simulations performed by Robbins and Wolden,[18] showing that the conductivity of a multilayer TCO structure approached that of a monolithic TCO film when well thicknesses were $\leqslant$5 nm. In general, it was not possible to achieve resistivities significantly lower than 10^{-3} Ω cm. This was due to the inability to transfer very high electron densities into the undoped ZnO layers for reasonable layer thicknesses, i.e., $>$1 nm. Also, the maximum average carrier density is reduced because only one of the three layers is doped. Thus, these materials will not compete directly with conventional TCOs in applications that require very low resistivities. However, they can provide superior transparency in moderately conductive layers because of the high mobilities that can be achieved. Modulation doping also offers the possibility of creating a high-mobility two-dimensional electron gas (2DEG), which will be important in all-transparent electronics to improve device speeds.[3,4,11]

The present results apply specifically to the ZnMgO system. However, they can be extended to make general predictions about other multilayer TCOs. The general characteristics that will make for a good modulation-doped TCO are as follows: (1) The doped layer should have the ability to be heavily doped; (2) the undoped layer should have the highest possible mobility; and (3) there should be a large conduction-band offset. One possible candidate for the undoped layer is CdO, where a mobility of 600 cm^2/V s has been reported.[10] Although this material has a band gap that is too small to be a good TCO on its own, in a thin layer the quantum-size effect would increase the effective band gap, improving transparency. CdO also exhibits a large Burstein-Moss effect,[10] which should increase the effective band gap when electrons are transferred from the wide band-gap layers.

The following discussion concerns the assumptions used regarding mobility values in the calculations. One of the key features in a modulation-doped structure is the intrinsic spacer layer, which physically separates the 2DEG from the ionized impurities. The choice to include an intrinsic ZnMgO spacer layer in the simulations was based on theoretical and

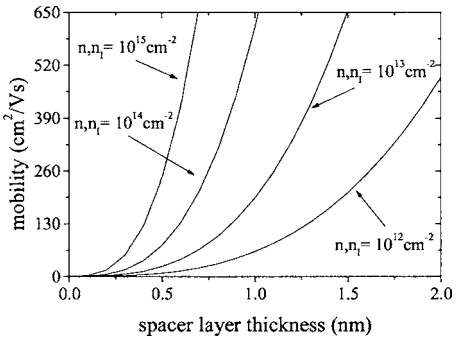

FIG. 6. Remote ionized impurity scattering mobility as a function of spacer layer thickness and electron/ion sheet concentration.

experimental results for GaAs/AlGaAs modulation-doped structures. Previous simulations on multilayer TCOs did not include an undoped spacer layer in their calculations.[18] The presence of the spacer layer, which minimizes electron wavefunction overlap into the doped layers, makes the assumption of $\mu=200$ cm^2/V s in the ZnO layers more realistic. However, this depends on a correct choice of the ZnMgO layer thickness. This choice is discussed further below.

Simulations were performed to compare the electron wave-function widths in ZnO/ZnMgO and GaAs/AlGaAs quantum wells. In both cases the quantum well was 2-nm thick, the donor concentration was 1×10^{19} cm^{-3}, the conduction-band offset was 0.25 eV, and there was only one confined state in the quantum well. The barrier layers in each simulation were made sufficiently thick so that boundary effects did not influence the calculation near the quantum well. The wave function in the ZnO system attenuates within ~1.5 nm of the quantum well, whereas in the GaAs system the wave function extends ~7 nm into the barrier region. The larger extent of the wave function in GaAs is a result of the much lower electron effective mass ($0.067m_e$ for GaAs and $0.094m_e$ for $Al_{0.324}Ga_{0.676}As$ compared to ZnO ($0.38m_e$ for ZnO and $1.5m_e$ for $Zn_{0.8}Mg_{0.2}O$). The simulation for GaAs/AlGaAs agrees very well with experimental data for GaAs/AlGaAs quantum wells, which show a mobility maximum at a spacer layer thickness between 5 and 7 nm.[29] This result suggests that a 1.5-nm ZnMgO spacer layer effectively separates the electron wave function from the ionized impurities.

A more quantitative calculation considers the effect of spacer layer thickness on the mobility of the 2DEG limited by remote ionized impurity scattering μ_{2d} given by[30,31]

$$\mu_{2d}=\frac{16\sqrt{2\pi}ed^3n^{3/2}}{\hbar n_I}, \tag{1}$$

where e is the electric charge, d is the spacing between the two-dimensional (2D) sheet of electrons (n cm^{-2}) and the 2D sheet of ionized impurities (n_I cm^{-2}), and $\hbar$ is Plank's constant divided by 2π. The values for mobility calculated from Eq. (1) agree well with experimental results for GaAs/AlGaAs modulation-doped structures.[30] Figure 6 shows the mobility based only on this remote ionized impurity scattering mechanism, assuming $n=n_I$, and that only the first subband in the 2DEG is occupied. Figure 6 indicates

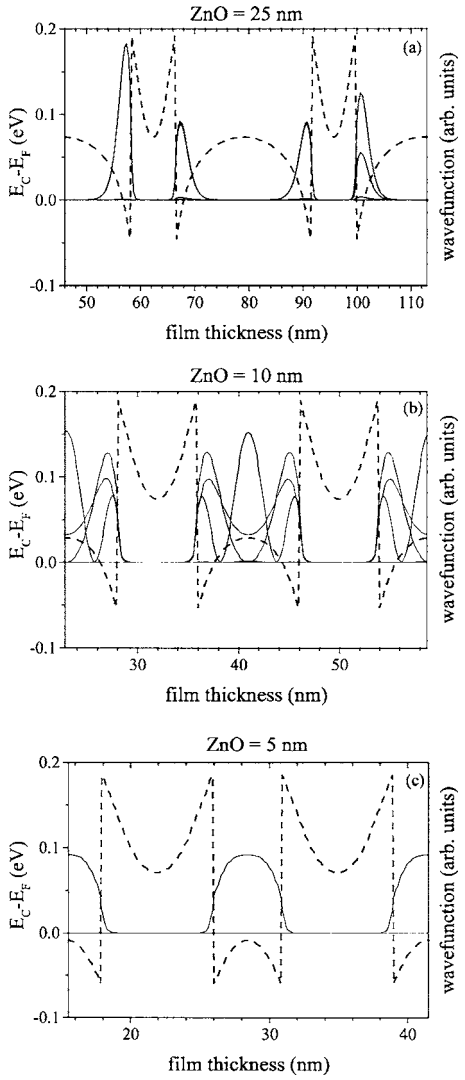

FIG. 7. Conduction-band energy diagrams (dashed lines) and the square of the electron wave functions for ZnO thicknesses of 25 (a), 10 (b), and 5 nm (c). The ZnMgO:Al thickness is 5 nm with a donor concentration of 1×10^{19} cm^{-3}, and the ZnMgO thickness is 1.5 nm.

that at the spacer layer thickness used in the simulations (1.5 nm) and the critical transferable electron sheet density (10^{13} cm^{-2}), the mobility limited by remote ionized impurity scattering is ~650 cm^2/V s, substantially higher than the bulk ZnO mobility of ~200 cm^2/V s which is limited by phonon scattering.

The success of a high-mobility 2DEG in ZnO/ZnMgO structures depends on finding a layer thickness and donor concentration that produces a single confined state per quantum well, thereby eliminating intersubband scattering.[31] Figure 7 shows the effect of ZnO thickness on the square of the electron wave function. For clarity, the conduction-band diagram is shown as a dashed line. Figure 7 shows two types of potential wells that exist in these structures. The first is the triangular-shaped well formed at the heterointerface due to band bending, the second is the quantum well formed in the entire ZnO layer as a result of the conduction-band offset between the layers. When the ZnO thickness is 25 nm all of the confined energy states lie within the triangular-shaped well at the heterointerface. At a ZnO thickness of 10 nm

quantized states reside both in the triangular-shaped well and within the well formed by the entire ZnO layer. When the ZnO thickness reaches 5 nm there are only states confined by the entire ZnO well, since the quantized energy levels are above the triangular wells at the interface. The transition from states being confined to the triangular well to states being confined to the entire ZnO layer as the ZnO thickness decreases is clearly shown. When the ZnO thickness is large [Fig. 7(a)] there are two triangular quantum wells per ZnO layer. Although the large ZnO thickness is not conducive to a low overall resistivity [Fig. 4(b)], it may be the best condition to produce a high-mobility 2DEG. At ZnO=10 nm [Fig. 7(b)] there is the possibility of extensive intersubband scattering, which may reduce the mobility.[31,32] When the ZnO layer is 5 nm it may be possible to achieve low resistivity and a high-mobility 2DEG at the same time since there is only one confined state per quantum well [Fig. 7(c)].

The simulations in this work assume the ability to grow highly perfect, lattice-matched epitaxial films with the desired purity and dopant levels. According to Gossard and Pinczuk the criteria for successful modulation doping are (1) absence of scattering centers in the conducting channel regions, (2) smooth and pure interfaces bounding these regions, (3) minimization of traps and compensating centers in the barriers, and (4) separation of the dopant atoms from the channel regions.[31] The choice of the ZnMgO system with reasonable lattice match (0.3% lattice mismatch for 20% Mg)[22] reflects these requirements. Furthermore, oxide crystal growth technology has improved to the point where high-quality heterojunctions can be grown.[33–35] Nonetheless, most epitaxial ZnO films are grown on (0001) sapphire substrates in which there is an 18% lattice mismatch between film and substrate, introducing surface roughness and crystal imperfections. Finally, the ability to control the carrier concentrations in TCO films is always a challenge as a result of inherent nonstoichiometry, but recent work has shown that this is possible with ZnMgO.[19] Many TCO applications would require a polycrystalline modulation-doped structure. Thus, if modulation doping is successfully demonstrated in epitaxial films, investigations of polycrystalline films will be needed. The strong preference of ZnO to grow with a (0002) orientation and a columnar grain strucuture[36] may provide locally smooth interfaces necessary for electron transfer. The role of grain boundaries as electron traps and scattering centers may ultimately limit the attainable properties in polycrystalline films.

V. SUMMARY AND CONCLUSIONS

A one-dimensional Poisson/Schrödinger program was used to investigate the effect of layer thicknesses, donor concentration, and band-gap offset on the electrical properties of transparent conducting modulation-doped ZnO/ZnMgO multilayer structures. Mobilities as high as 145 $cm^2/V\,s$ were predicted for a structure with an average carrier density of 3.8×10^{18} cm^{-3} and a resistivity of 1×10^{-2} Ω cm; for a comparable resistivity in monolithic ZnO, the mobility would be lower $\sim$30 $cm^2/V\,s$ and the carrier density would be higher. The ability to confine conduction electrons to a 2DEG offers enhanced flexibility in the design of transparent electronics, allowing for the possibility of modulation-doped field-effect transistors. Thus, the modulation-doping approach is a possible means for enhancing TCO properties. However, it was found that the maximum sheet electron density that could be transferred from the doped to the undoped layers was $\sim10^{13}$ cm^{-2}, limiting the lowest resistivity to 1.5×10^{-3} Ω cm. The thickness ranges providing highest mobilities combined with low resistivity were 2–5 nm for the pure ZnO and 2–5 nm for the ZnMgO:Al. A pure ZnMgO set-back layer thickness of $\sim$1.5 nm was used in order to minimize the impact of remote ionized impurity scattering on mobility. The undoped ZnO layer thickness should be either small, $\leqslant$5 nm, or large, $\geqslant$25 nm, in order to avoid possible intersubband scattering.

ACKNOWLEDGMENTS

This work was supported by the MRSEC program of the National Science Foundation (DMR-0076097) at the Material Research Center of Northwestern University.

[1] T. Minami, T. Miyata, and T. Yamamoto, Surf. Coat. Technol. **109**, 583 (1998).
[2] B. Rech *et al.*, Sol. Energy Mater. Sol. Cells **74**, 439 (2002).
[3] K. Nomura, H. Ohta, K. Ueda, T. Kamiya, M. Hirano, and H. Hosono, Science **300**, 1269 (2003).
[4] J. F. Wager, Science **300**, 1245 (2003).
[5] S. Kim, B. S. Kang, F. Ren, Y. W. Heo, K. Ip, D. P. Norton, and S. J. Pearton, Electrochem. Solid-State Lett. **7**, G145 (2004).
[6] T. Minami, MRS Bull. **25**, 38 (2000).
[7] T. J. Coutts, D. L. Young, and X. Li, MRS Bull. **25**, 58 (2000).
[8] A. J. Freeman, K. R. Poeppelmeier, T. O. Mason, R. P. H. Chang, and T. J. Marks, MRS Bull. **25**, 45 (2000).
[9] T. J. Coutts, D. L. Young, X. Li, W. P. Mulligan, and X. Wu, J. Vac. Sci. Technol. A **18**, 2646 (2000).
[10] M. Yan, M. Lane, C. R. Kannewurf, and R. P. H. Chang, Appl. Phys. Lett. **78**, 2342 (2001).
[11] B. J. Norris, J. Anderson, J. F. Wager, and D. A. Keszler, J. Phys. D **36**, L105 (2003).
[12] I. A. Rauf, Mater. Lett. **18**, 123 (1993).
[13] K. Ellmer, J. Phys. D **33**, R17 (2000).
[14] R. Dingle, H. L. Stormer, A. C. Gossard, and W. Wiegmann, Appl. Phys. Lett. **33**, 665 (1978).
[15] T. J. Drummond, H. Morkoc, K. Hess, and A. Y. Cho, J. Appl. Phys. **52**, 5231 (1981).
[16] S. Gokden, Phys. Status Solidi A **200**, 369 (2003).
[17] C. H. Mueller, E. T. Croke, and S. A. Alterovitz, Electron. Lett. **39**, 1353 (2003).
[18] J. J. Robbins and C. A. Wolden, Appl. Phys. Lett. **83**, 3933 (2003).
[19] D. J. Cohen, K. C. Ruthe, and S. A. Barnett, J. Appl. Phys. **96**, 459 (2004).
[20] G. L. Snider, Free Ware program available at http://www.nd.edu/~gsnider/.
[21] I. H. Tan, G. L. Snider, L. D. Chang, and E. L. Hu, J. Appl. Phys. **68**, 4071 (1990).
[22] A. Ohtomo *et al.*, Appl. Phys. Lett. **72**, 2466 (1998).
[23] H. Ryoken, Y. Adachi, I. Sakaguchi, N. Ohashi, H. Haneda, and T. Takenaka, *Electroceramics in Japan VI (2003)*, Vol. 248 of Key Engineering Materials (Trans Tech Publications, Zurich, 2003), pp. 103–106.
[24] W. R. L. Lambrecht, S. Limpijumnong, and B. Segall, MRS Internet J. Nitride Semicond. Res. **4**, G6.8 (1999).
[25] P. Boieriu, R. Sporken, and S. Sivananthan, J. Vac. Sci. Technol. B **20**, 1777 (2002).
[26] K. Ellmer, J. Phys. D **34**, 3097 (2001).
[27] K. Matsubara, H. Tampo, H. Shibata, A. Yamada, P. Fons, K. Iwata, and S. Niki, Appl. Phys. Lett. **85**, 1374 (2004).
[28] S. D. Lazarev, E. Z. Meilikhov, and B. A. Aronzon, in *Handbook of Physical Quantities*, edited by I. S. Grigoriev, E. Z. Meilikhov, and A. A. Radzig (CRC, New York, 1997).

[29]T. J. Drummond, H. Morkoc, and A. Y. Cho, J. Appl. Phys. **52**, 1380 (1981).
[30]P. J. Price, Surf. Sci. **113**, 199 (1982).
[31]A. C. Gossard and A. Pinczuk, in *Synthetic Modulated Structures*, edited by L. L. Chang and B. C. Giessen (Academic, Orlando, 1985).
[32]P. T. Coleridge, Semicond. Sci. Technol. **5**, 961 (1990).
[33]D. G. Schlom, J. H. Haeni, J. Lettieri, C. D. Theis, W. Tian, J. C. Jiang, and X. Q. Pan, Mater. Sci. Eng., B **87**, 282 (2001).
[34]H. D. Sun, T. Makino, Y. Segawa, M. Kawasaki, A. Ohtomo, K. Tamura, and H. Koinuma, J. Appl. Phys. **91**, 1993 (2002).
[35]T. Gruber, C. Kirchner, R. Kling, F. Reuss, and A. Waag, Appl. Phys. Lett. **84**, 5359 (2004).
[36]L. J. Meng and M. P. Dossantos, Vacuum **46**, 1001 (1995).
[37]H. L. Hartnagel, A. L. Dawar, A. K. Jain, and C. Jagadish, *Semiconducting Transparent Thin Films* (IOP, London, 1995).